Special Technical Report 33

MEASUREMENTS OF EQUATORIAL MAGNETIC DIP ANGLE AT IONOSPHERIC HEIGHTS

By VICHAI T. NIMIT

Prepared for:

U.S. ARMY ELECTRONICS COMMAND
FORT MONMOUTH, NEW JERSEY 07703

CONTRACT DA-36-039 AMC-00040(E)
ORDER NO. 5384-PM-63-91

STANFORD RESEARCH INSTITUTE

MENLO PARK, CALIFORNIA

DISCLAIMER NOTICE

THIS DOCUMENT IS THE BEST QUALITY AVAILABLE.

COPY FURNISHED CONTAINED A SIGNIFICANT NUMBER OF PAGES WHICH DO NOT REPRODUCE LEGIBLY.

STANFORD RESEARCH INSTITUTE
MENLO PARK, CALIFORNIA

May 1967

Special Technical Report 33

MEASUREMENTS OF EQUATORIAL MAGNETIC DIP ANGLE AT IONOSPHERIC HEIGHTS

Prepared for:

U.S. ARMY ELECTRONICS COMMAND
FORT MONMOUTH, NEW JERSEY 07703

CONTRACT DA-36-039 AMC-[illegible]40(E)
ORDER NO. 5384-PM-63-01

By: VICHAI T. NIMIT

SRI Project 4240

Approved: E. L. YOUNKER, TECHNICAL DIRECTOR
MRDC ELECTRONICS LABORATORY BANGKOK

W. R. VINCENT, MANAGER
COMMUNICATION LABORATORY

D. R. SCHEUCH, EXECUTIVE DIRECTOR
ELECTRONICS AND RADIO SCIENCES

Spansored by
ADVANCED RESEARCH PROJECTS AGENCY
ARPA ORDER 371

Copy No. 158

ABSTRACT

Data collected for calculating electron content of the ionosphere by the Faraday rotation technique can be used to calculate the magnetic dip angle at ionospheric heights near the geomagnetic dip equator. In this report the magnetic dip angle at ionospheric height was determined at the position where the angle between the ray path from the satellite to the ground station and the geomagnetic field vector is 90° (transverse position).

The magnetic dip angle calculation was based on the assumption of a constant height of 350 km for the centroid of the ionospheric electron-density profile. The spherical harmonic analysis is used to verify the experimental results. The results compare well with the surface magnetic dip angle, measured in 1956-1966 by the Geodesy Department of the Ministry of Defense, Thailand, and indicate that the magnetic dip angle at ionospheric height is very close to the surface value.

These data permit estimation of the position of the geomagnetic dip equator at the ionospheric height. The estimated position of this equator is directly above the geographic latitude of 9.30°N. This latitude intersects the southern peninsula of Thailand about 480 km south of Bangkok (near Surat Thani). This estimated value compares well with the surface geomagnetic dip equator and indicates that the dipole field is a good model for Southeast Asia in the vicinity of longitude 100°E.

BLANK PAGE

CONTENTS

ILLUSTRATIONS

TABLES

ACKNOWLEDGMENTS

Faraday rotation observations are being carried out in Thailand by the Electronics Laboratory of the Military Research and Development Center at Bangkok, Thailand, a joint Thailand-United States organization. The cooperation and participation of the staff of the Thailand Ministry of Defense and the support of the United States Advanced Research Projects Agency and the United States Army Electronics Command have made possible the accumulation of the data analyzed in this report.

The author gratefully acknowledges the assistance of various individuals who have made significant contributions to this study. David J. Lyons, John W. Chapman, Jan van der Laan, and Uthai Mungtrisan participated in the operation of the equipment, Prajuab Nimityongskul supervised the data reduction, and Pibul Sinthavalai assisted in the data reduction. Thanks are due Lt. Cdr. Paibul Nacaskul (Royal Thai Navy) for helpful discussions and George Hagn for suggesting and encouraging this study. Goddard Space Flight Center, National Aeronautics and Space Administration, supplied the Satellite S-66 ephemeris data.

I INTRODUCTION

The Electronics Laboratory of the Military Research and Development Center (MRDC) Bangkok, Thailand was set up as a joint Thailand-United States organization for the study of communication problems in equatorial areas. One of the major objectives of communication research in equatorial areas is the study of the ionosphere. To increase understanding of the ionospheric characteristics, records of the Faraday rotation on 40- and 41-MHz signals from the S-66 (EXPLORER 22) radio beacon satellite have been accumulated at the Bangkok MRDC Electronics Laboratory,[1,4*] and at four remote sites located north and south of Bangkok. The projection of a typical satellite path on the earth over these sites is shown in Fig. 1. Thus data for sites in the range of geographic latitude between about 7°N and 19°N were collected.

Data collected for calculating electron content of the ionosphere by the Faraday rotation technique can be used to calculate the magnetic dip angle above the earth's surface near the magnetic equatorial region. The application of this technique will help in locating the geomagnetic dip equator, which passes through Thailand to the south of Bangkok. The technique provides information for comparison of the above-surface magnetic dip angle with the surface magnetic dip angle available from measurements taken at the earth's surface in Thailand,[5] with other published values,[6,7] and with the theoretical value based on the spherical harmonic analysis. Thus this work will aid in studying radio propagation effects related to geomagnetic control of the ionosphere that are important to communication in Southeast Asia. For example, consideration of the magnetoionic theory led Hagn to explore the optimum orientation for linearly polarized antennas used on short ionospheric paths near the geomagnetic dip equator.[8] The present work will permit a better estimate of where to use linear antenna (*e.g.*, dipole) orientation and where a diversity scheme based on antenna orientation will work (owing to the effects of the earth's magnetic field in the ionosphere). This work also provides information for studying the geomagnetic controlled HF spectrum, and that can be used to determine where post-sunset spread-*F* conditions are most likely to occur and hence cause HF communication outage.

* References are listed at the end of the report.

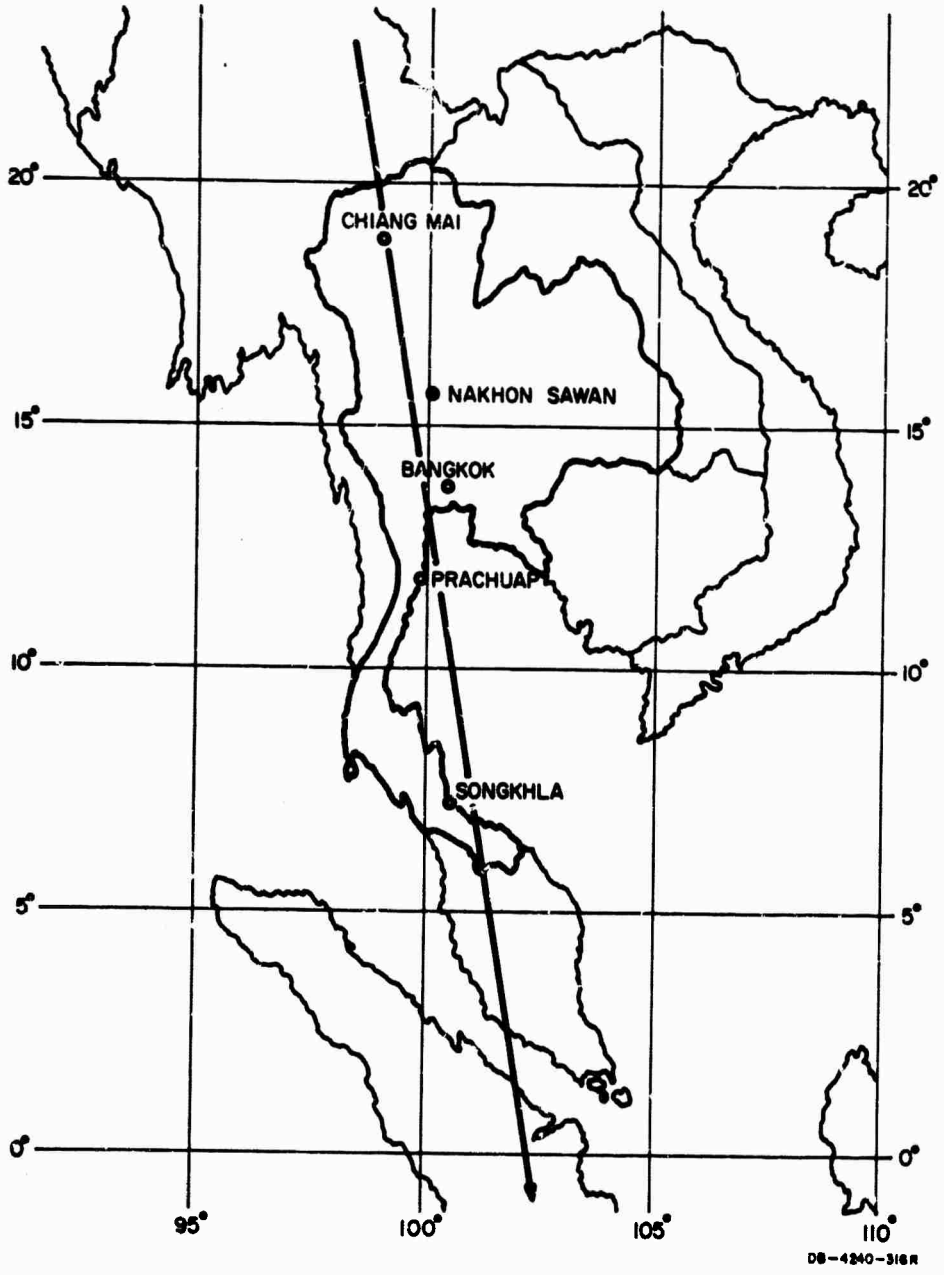

FIG. 1 LOCATIONS OF SATELLITE RECEIVING SITES

This report presents the method of calculations and results for selected Faraday rotation data from satellite passes observed by the receiving stations. The assumptions involved in calculations are given and the possible source. of error are discussed.

BLANK PAGE

II THEORETICAL BACKGROUND

When an electromagnetic wave propagates through the ionosphere from a satellite, its resultant polarization progressively rotates, under the influence of the magnetic field,[9] and this phenomenon is called Faraday rotation. Figure 2 illustrates the concept of Faraday rotation. The satellite is shown in three positions ($\theta > 90°$, $\theta = 90°$, and $\theta < 90°$, where θ is the angle between the signal ray path and the earth's magnetic field), and the ionosphere between the satellite and the ground station is indicated. The centroid height of the ionospheric electron density profile is shown as h_c. At one time during the passage of the satellite, the signal ray path is perpendicular to the magnetic field ($\theta = 90°$). Satellite transit of this unique point, called the transverse position T_0, usually leaves a visible signature on the Faraday rotation fading records for stations located near the geomagnetic equator. An example of such a signature is shown on the fading record of Fig. 3.

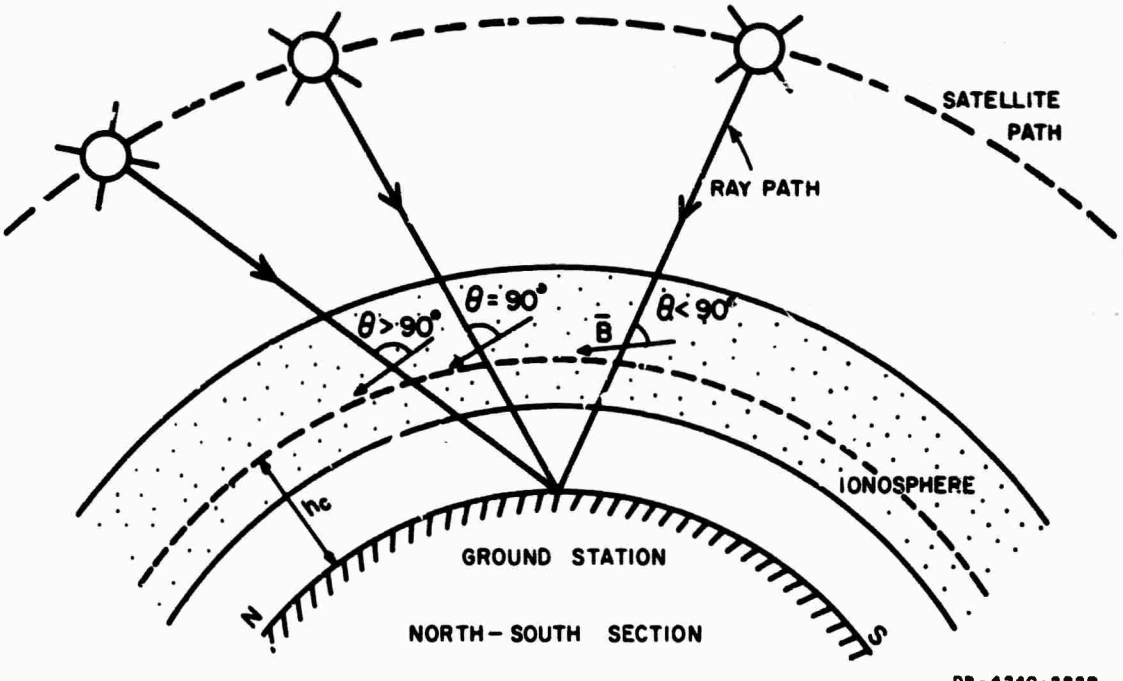

FIG. 2 FARADAY ROTATION GEOMETRY

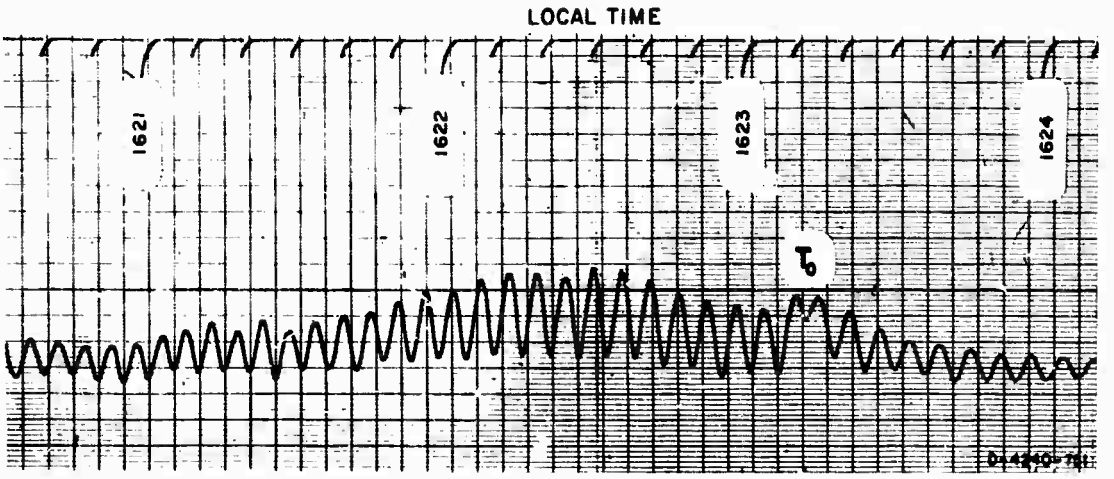

FIG. 3 SAMPLE OF SATELLITE FADING RECORD

By using the satellite ephemeris data for satellite position information and the observed time of T_0, it is possible to calculate the magnetic dip angle from magnetic-field and ray-path geometry considerations. The value of dip angle thus obtained is considered to apply at a certain height in the ionosphere. This height is chosen by the following considerations: The electron-density distribution profile of the ionosphere based on the Chapman-type distribution has found wide use in modeling the topside ionosphere. Although several very questionable assumptions were made in the derivation of Chapman's formula, the general shape of the electron-density distribution with altitude as given by Chapman's equation still gives a reasonable fit of the actual distribution profile as we know it.[10] From the shape of the ionospheric electron-density distribution it is assumed that most of the Faraday rotations occur near the peak of this distribution in the *F* layer.[9,11] This study assumes, as other studies have, that the main effect of the earth's magnetic field is localized near the centroid of the electron-density profile.[11,12] The centroid height for the area of interest is obtained by fitting the Faraday rotation electron content data to a Chapman model of the ionosphere. So the centroid height in the ionosphere is determined to be at a level approximately 50 km above the height of maximum density,[9,11] which can be determined from a true-height analysis of vertical-incidence ionograms obtained near the location and time of the satellite passages.

III MAGNETIC DIP ANGLE CALCULATION

The purpose of this section is to describe the method of calculation of magnetic dip angle at ionospheric heights near the geomagnetic equatorial region.

The Faraday rotation technique used to determine the magnetic dip angle at the centroid height of the ionospheric electron density profile was applied at the position where the T_0 (transverse position) occurred. As illustrated in Fig. 3, the local time* was recorded on the chart to relate the observed data to the physical position of the satellite in its orbit. The unique point, T_0, is plainly visible in this chart. The satellite position and height at the time corresponding to T_0 can be obtained from ephemeris data provided by the U.S. National Aeronautics and Space Administration (NASA).

For the calculations of this section the wave frequency was assumed to be so high that refraction can be neglected (that is, the wave frequency is much higher than the maximum plasma and collision frequencies). A profile view of the satellite and the ground station is shown in Fig. 4. It can be seen that the coordinates of the sub-satellite point (the projection of satellite on the earth), the sub-ionospheric point (the projection on the earth of the intersection of the ray path between satellite and ground station with the centroid of the ionospheric electron density profile) and ground station are θ_s, λ_s; θ_i, λ_i; θ_r, λ_r; geographic latitude and longitude, respectively. The satellite height is h_s. The earth's radius is denoted by R_e and the ionospheric centroid height is h_c.

At the position where the signal ray path from the satellite is perpendicular to the geomagnetic field (T_0 position), the magnetic dip angle, I_B, at the ionospheric centroid height can be calculated from the expressions given by the following:

$$I_B = \tan^{-1} (\cot I_R \cos D_R)^{\dagger} \qquad (1)$$

* Local time was established using a General Radio 1115B Frequency Standard adjusted using phase referenced to the VLF transmission from GBR in England on 16 kHz. Time ticks generated by a GR 1123A Synchronometer from this standard were compared daily with time transmissions from WWVH and JJY on 10 and 15 MHz. The resulting time estimate is accurate to ±5 milliseconds.

† The derivation is given in Appendix A.

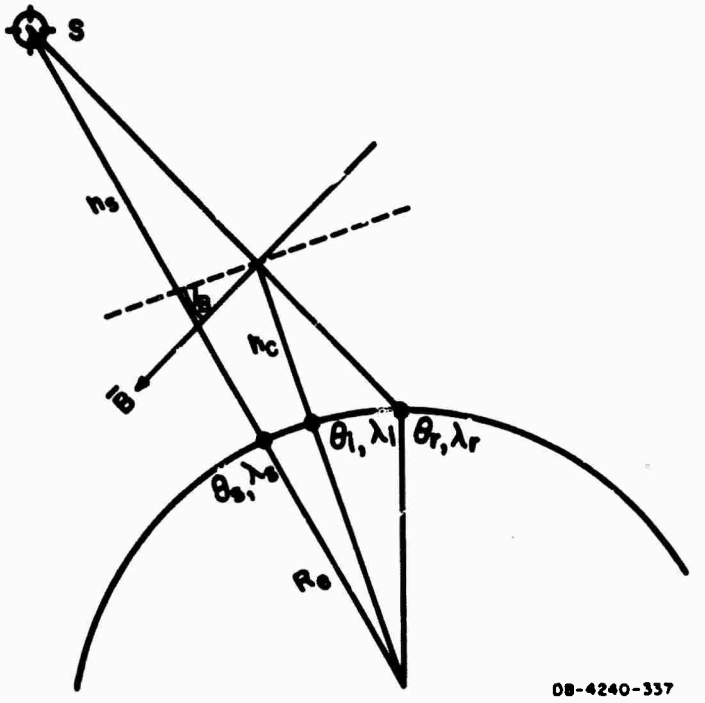

FIG. 4 GEOMAGNETIC FIELD — RAY PATH PROFILE

$$\cot I_R = \frac{R_e(R_e + h_s)\sin C}{\{(R_e + h_c)^2[R_e^2 + (R_e + h_s)^2 - 2R_e(R_e + h_s)\cos C] - [R_e(R_e + h_s)\sin C]^2\}^{1/2}} \tag{2}$$

$$\cos D_R = \frac{\sin \theta_s}{\cos \theta_i \sin (C - b)} - \tan \theta_i \cot (C - b) \tag{3}$$

where

$$C = \cos^{-1}[\sin \theta_s \sin \theta_r + \cos \theta_s \cos \theta_r \cos (\lambda_s - \lambda_r)] \tag{4}$$

$$b = \cos^{-1}\left[\frac{R_e(R_e + h_s)\sin C}{(R_e + h_c)[R_e^2 + (R_e + h_s)^2 - 2R_e(R_e + h_s)(\cos C)]^{1/2}}\right]$$

$$- \cos^{-1}\left[\frac{(R_e + h_s)\sin C}{[R_e^2 + (R_e + h_s)^2 - 2R_e(R_e + h_s)\cos C]^{1/2}}\right] \tag{5}$$

$$\theta_i = \sin^{-1}\left[\sin\theta_r(\cos b - \sin b \cot C) + \sin\theta_s \sin b \operatorname{cosec} C\right] \quad . \quad (6)$$

The magnetic dip angle obtained from Eq. (1) for the ionospheric centroid height corresponds to the sub-ionospheric point, θ_i and λ_i. The sub-ionospheric latitude, θ_i, can be obtained from Eq. (6), and the sub-ionospheric longitude, λ_i, can be calculated by the following equations:

$$N = \sin^{-1}\left\{\frac{\sin b}{\cos\theta_i}\left[1 - \left(\frac{\sin\theta_s - \sin\theta_r\cos C}{\cos\theta_r \sin C}\right)^2\right]^{1/2}\right\} \quad (7)$$

if

$$\lambda_s \geq \lambda_r, \quad \text{then} \quad \lambda_i = \lambda_r + N \quad (8)$$

$$\lambda_s \leq \lambda_r, \quad \text{then} \quad \lambda_i = \lambda_r - N \quad . \quad (9)$$

These relationships between the satellite and the ground station at the T_0 position can be used to calculate the magnetic dip angle at the ionospheric centroid height from the experimentally obtained Faraday rotation data.

BLANK PAGE

IV SPHERICAL HARMONIC MODEL CALCULATION

The geomagnetic field can be represented theoretically by mathematical functions.[7,13] The spherical harmonic expansion is chosen to represent a theoretical model of the earth's magnetic field, since its functions are suitable for the mathematic expression of arbitrary distributions on the surface of any sphere.

The spherical harmonic function to be considered here to serve for the earth's magnetic field representation is based on several basic assumptions, since the fundamental causes for the earth's field have not been satisfactorily explained. Gauss[13] assumed that there is no magnetic matter near the ground and no electric current passing from the atmosphere to the ground. Hence, if we assume that there is no external source, all the currents producing the magnetic field are inside the earth's surface. Then in any solution to find the distribution of magnetic field in the region that contains no current, the curl of the magnetic field vector, $\bar{B}$, at any point must (by Maxwell's equation) be zero:

$$\nabla \times \bar{B} = 0 \quad . \tag{10}$$

This equation implies the existence of the gradient of the magnetic potential function, ϕ, as

$$\bar{B} = -\nabla\phi \quad . \tag{11}$$

By Maxwell's equation, the divergence of $\bar{B}$ is identically zero:

$$\nabla \cdot \bar{B} = 0 \quad . \tag{12}$$

Substituting Eq. (11) into Eq. (12) the magnetic potential function satisfies Laplace's equation:

$$\nabla^2\phi = 0 \quad . \tag{13}$$

The solutions of this equation in spherical coordinates are known as spherical harmonic functions.[13,14] Figure 5 shows the spherical coordinate system, colatitude ($\bar{\theta}$) increasing southward, longitude (λ) increasing eastward, and radial distance (a) increasing outward. The magnetic potential function at any point can be expressed as:

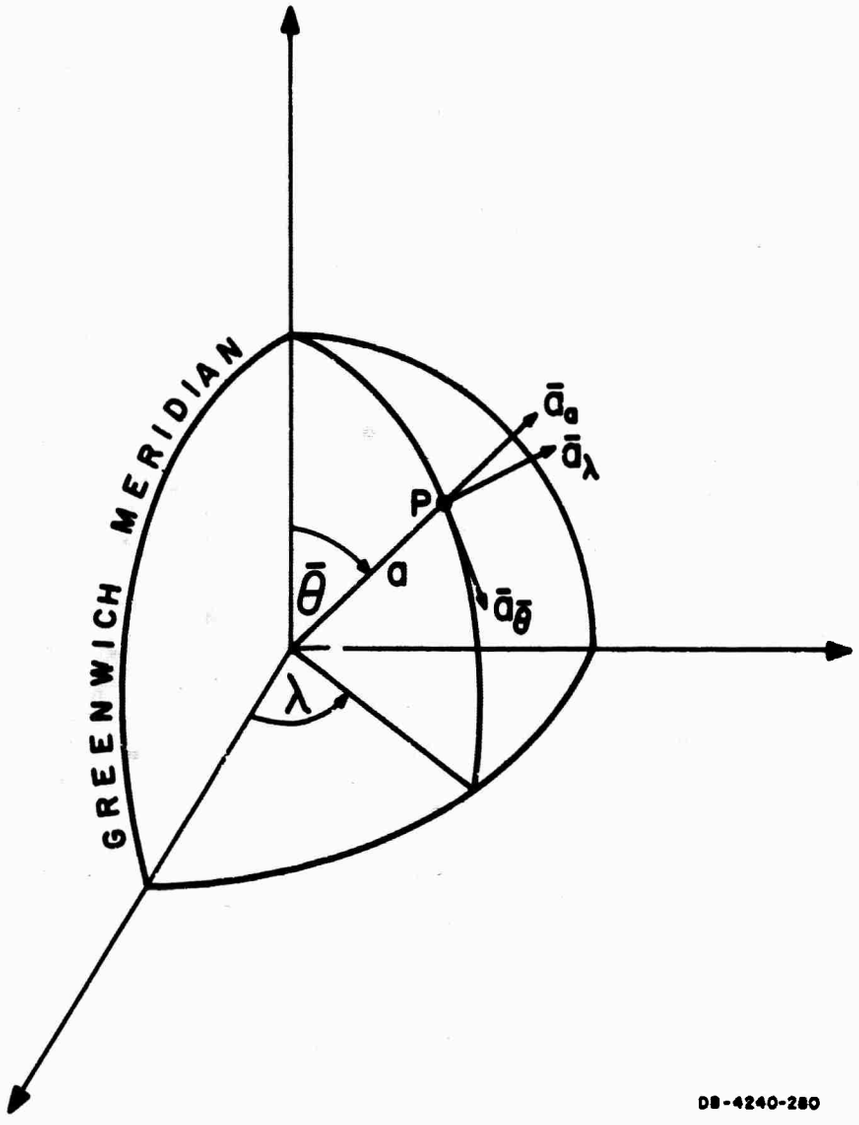

FIG. 5 SYSTEM OF SPHERICAL COORDINATES

$$\phi = R_e \sum_{n=1}^{\infty} \sum_{m=1}^{n} \left(\frac{R_e}{a}\right)^{n+1} P_n^m(\cos \bar{\theta})(A_n^m \cos m\lambda + B_n^m \sin m\lambda) \quad . \qquad (14)$$

Here R_e denotes the radius of the earth (equal to 6370 km); A_n^m and B_n^m are the numerical harmonic coefficients; and $P_n^m(\cos \bar{\theta})$ is the Schmidt orthogonal function of degree n and order m with $m \leq n \geq 1$. The Schmidt function can be expressed as numerical multiples of the associated Legendre polynomial, $P_{n,m}(\cos \bar{\theta})$, as

$$P_n^m(\cos \bar{\theta}) = \begin{cases} P_{n,m}(\cos \bar{\theta}) & \text{when } m = 0 \\ \left[\frac{2(n-m)!}{(n+m)!}\right]^{1/2} \cdot P_{n,m}(\cos \bar{\theta}) & \text{when } m > 0 \end{cases}$$

where $P_{n,m}(\cos \bar{\theta})$ is expressed in a finite series, as follows:

$$P_{n,m}(\cos \bar{\theta}) = \frac{(2n)!}{2^n(n)! \cdot (n-m)!} \sin^m \bar{\theta} \left[\cos \bar{\theta}^{n-m} - \frac{(n-m)(n-m-1)}{2(2n-1)} \cos^{n-m-2} \bar{\theta} + \frac{(n-m)(n-m-1)(n-m-2)(n-m-3)}{2(4)(2n-1)(2n-3)} \cos^{n-m-4} \bar{\theta} \ \ldots \right] . \qquad (15)$$

By Eq. (11) the magnetic induction can be written by the differential equation

$$\bar{B} = -\left(\bar{a}_a \frac{\partial \phi}{\partial a} + \frac{\bar{a}_{\bar{\theta}}}{a} \frac{\partial \phi}{\partial \bar{\theta}} + \frac{\bar{a}_\lambda}{a \sin \bar{\theta}} \frac{\partial \phi}{\partial \lambda}\right) \quad . \qquad (16)$$

The earth's magnetic induction, $\bar{B}$, at any point is a vector and its modulus is called total intensity or total field. It is noted that the earth's magnetic field has been tacitly treated mathematically as if it were constant in time. This total field is defined usually by the Cartesian components as positive to the northward component (X), eastward component (Y), and downward component (Z), as shown by the coordinates of point P in Fig. 5.

Hence, the Cartesian components of total field can be obtained:

$$X = \frac{1}{a}\frac{\partial \phi}{\partial \bar{\theta}}$$

$$Y = -\frac{1}{a \sin \bar{\theta}}\frac{\partial \phi}{\partial \lambda} \qquad (17)$$

$$Z = \frac{\partial \phi}{\partial a} \quad .$$

The total field can be obtained by $B = (H^2 + Z^2)^{1/2}$ where $H = (X^2 + Y^2)^{1/2}$. The magnetic dip angle I_B = arc tan Z/H.

The spherical harmonic function was calculated using the CDC-3100 electronic computer. The program was performed for the first six harmonics using the spherical harmonic coefficients available to the author.[15] Figure 6 shows a typical plot of the computed total field decreasing with the increasing of the higher degree of n at Bangkok. The ratio $(R_e/a)^{n+1}$ in Eq. (14) is the altitude decay factor. This factor indicates the decrease of total field with the increase of altitude; the greater the altitude up to the height of ionosphere, $a = R_e + h_c$, the higher the degree of n that can be neglected.

Values of magnetic dip angle computed at various altitudes over the receiving stations are shown in Table I. These results show that the magnetic dip angle even at an altitude of 400 km is very close to the surface values. Figure 7 presents a map of the surface magnetic dip angle of Thailand prepared from this computer program. The spherical harmonic equations of magnetic field components for the first six harmonics are shown in detail in Appendix B.

Table I

COMPUTED MAGNETIC DIP ANGLE

	LOCATION		MAGNETIC DIP ANGLE			
	Longitude	Latitude	Surface Value	h_c = 300 km	h_c = 350 km	h_c = 400 km
Chiang Mai	98.97°E	18.82°N	22.32°N	22.13°N	22.10°N	22.06°N
Nakhon Sawan	100.18°E	15.66°N	14.98°N	14.88°N	14.86°N	14.84°N
Bangkok	100.57°E	13.73°N	10.31°N	10.30°N	10.29°N	10.28°N
Prachuap	99.80°E	11.80°N	5.91°N	5.90°N	5.90°N	5.90°N
Songkhla	100.62°E	7.20°N	4.96°S	4.87°S	4.86°S	4.85°S

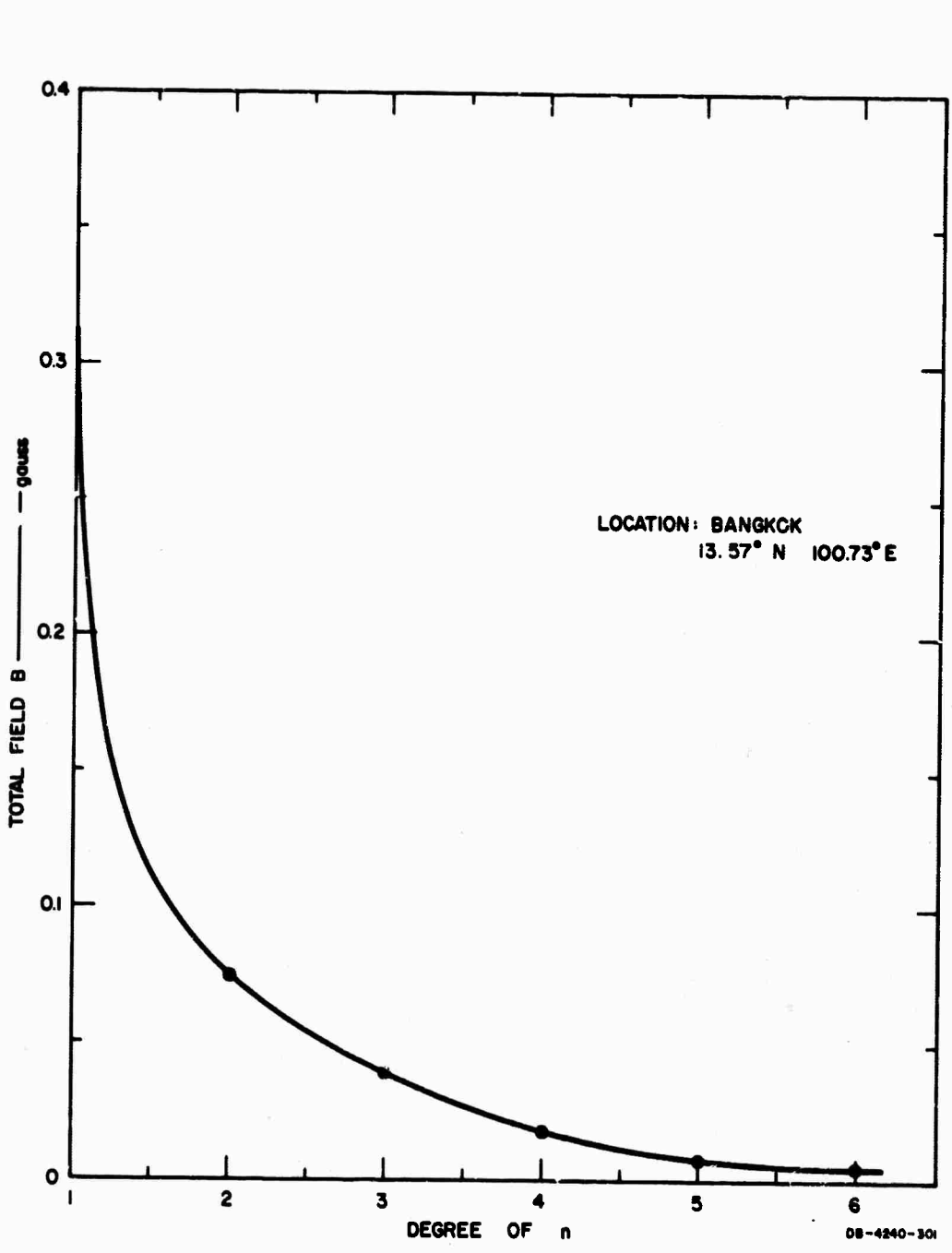

FIG. 6 TOTAL FIELD AS FUNCTION OF n AT BANGKOK

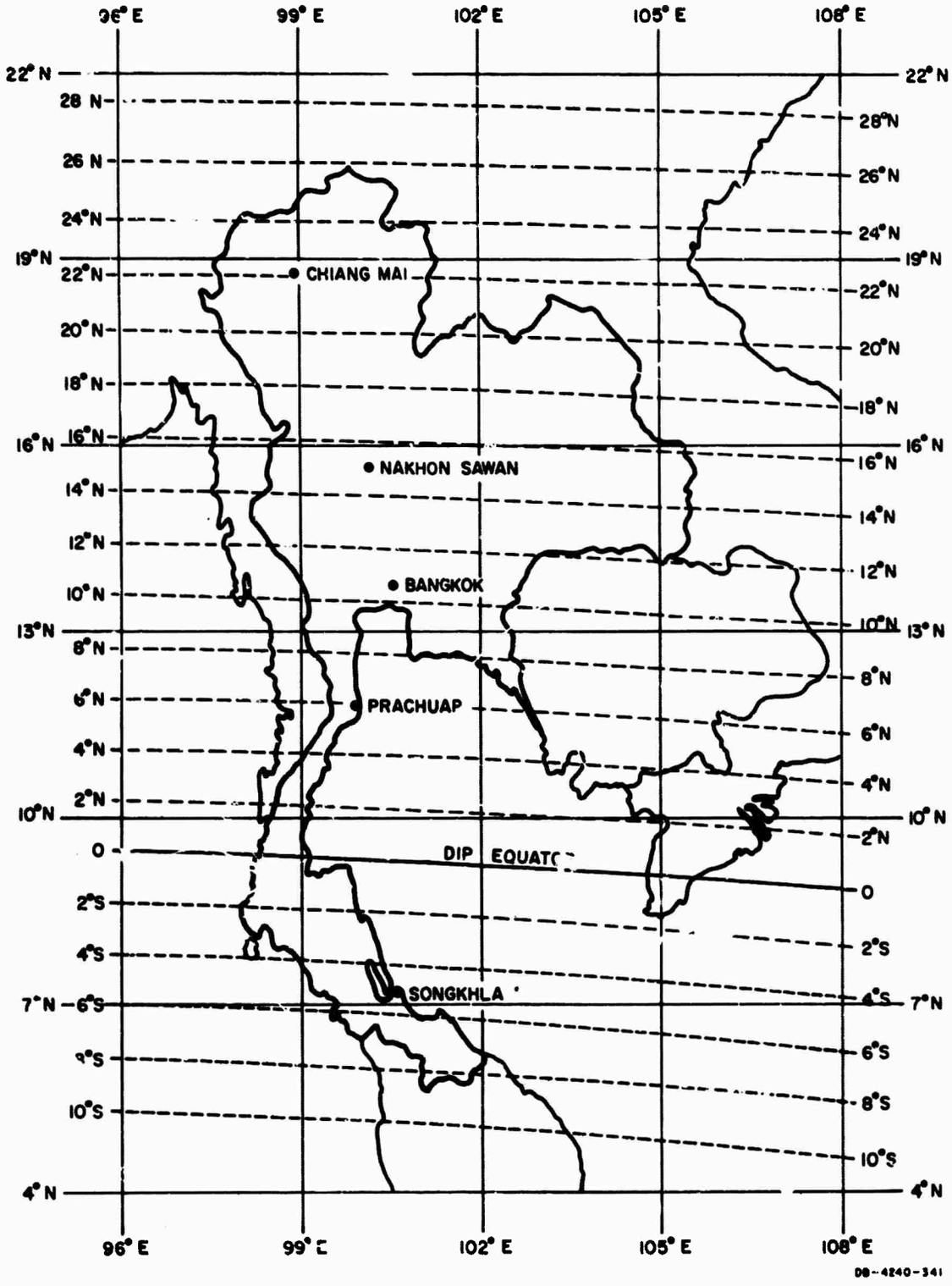

FIG. 7 MAP OF COMPUTED MAGNETIC DIP ANGLE

V RESULTS

A. Transverse Position Magnetic Dip Angle

The magnetic dip angle over each receiving site was calculated at the position where T_0 occurs. The magnetic dip angle was assumed to apply at the centroid height of the ionospheric profile (h_c approximately 350 km). This height appears to be realistic from a limited amount of true-height analysis performed on typical daytime and nighttime ionograms at Bangkok.[16]

The results of the magnetic dip angle calculations from Faraday rotation observations of five receiving sites are shown in Tables II through VI. The mean and variance values are summarized in Table VII. The mean values of magnetic dip angle are plotted in Fig. 8. This figure represents the magnetic dip angle at the altitude of 350 km over the range of geographic latitude between about 6° to 21°N near the 100°E longitude.

Table II

MAGNETIC DIP ANGLE AT ALTITUDE 350 km OVER GEOGRAPHIC LOCATION 20.33°N , 99.21°E (CHIANG MAI SITE DATA)

DATE	SATELLITE REVOLUTION NUMBER	TRANSVERSE POSITION (T_0) LOCAL TIME	MAGNETIC DIP ANGLE
29 Nov 1966	10724A*	2048:15	25.42°N
2 Dec 1966	10765A	2025:12	25.38°N
8 Dec 1966	10847A	1939:21	25:46°N
15 Jan 1967	11365A	1413:46	25.53°N
18 Jan 1967	11406A	1350:53	25.54°N
21 Jan 1967	11447A	1327:58	25.41°N
26 Jan 1967	11508D*	0043:05	25.53°N
27 Jan 1967	11529A	1242:10	25.52°N

* The letters A and D indicate ascending and descending (north- and south-going) satell passes, respectively.

Teble III

MAGNETIC DIP ANGLE AT ALTITUDE 350 km OVER GEOGRAPHIC LOCATION 16.58°N, 100.60°E (NAKHON SAWAN SITE DATA)

DATE	SATELLITE REVOLUTION NUMBER	TRANSVERSE POSITION (T_0) LOCAL TIME	MAGNETIC DIP ANGLE
28 Oct 1966	10272A	0059:56	16.67°N
29 Oct 1966	10299D	1237:12	16.49°N
31 Oct 1966	10313A	0036:57	16.62°N
3 Nov 1966	10354A	0013:57	16.43°N
4 Nov 1966	10374D	1151:23	16.56°N
5 Nov 1966	10395A	2350:57	16.64°N
8 Nov 1966	10436A	2327:56	16.66°N
11 Nov 1966	10477A	2304:57	16.65°N

Table IV

MAGNETIC DIP ANGLE AT ALTITUDE 350 km OVER GEOGRAPHIC LOCATION 14.38°N, 100.60°E (BANGKOK SITE DATA)

DATE	SATELLITE REVOLUTION NUMBER	TRANSVERSE POSITION (T_0) LOCAL TIME	MAGNETIC DIP ANGLE
25 Dec 1964	105IA	2126:23	12.02°N
10 Feb 1965	1693A	1456:42	12.70°N
18 Sept 1965	4712A	0842:40	12.07°N
27 Oct 1965	5251D	1459:22	12.25°N
30 Oct 1965	5292D	1436:35	12.24°N
5 Nov 1965	5374D	1351:11	12.05°N
8 Nov 1965	5415D	1328:13	12.13°N
10 Nov 1965	5436A	0125:26	12.67°N
13 Nov 1965	5477A	0102:43	12.64°N
16 Nov 1965	5518A	0039:59	12.77°N
22 Nov 1965	5600A	1654:31	12.68°N
13 Jan 1966	6324A	1637:01	12.00°N
16 Jan 1966	6365A	1614:23	12.11°N
16 Mar 1966	7171A	0809:49	12.24°N

Table V

MAGNETIC DIP ANGLE AT ALTITUDE 350 km OVER GEOGRAPHIC LOCATION 12.14°N, 100.47°E (PRACHUAP SITE DATA)

DATE	SATELLITE REVOLUTION NUMBER	TRANSVERSE POSITION (T_0) LOCAL TIME	MAGNETIC DIP ANGLE
4 June 1966	8270D	0838:18	6.20°N
7 June 1966	8311D	0815:33	6.17°N
9 June 1966	8346A	2039:35	6.20°N
12 June 1966	8387A	2016:39	6.50°N
19 June 1966	8475D	0644:12	5.95°N
20 June 1966	8496A	1840:56	6.37°N
22 June 1966	8516D	0621:22	6.00°N
23 June 1966	8537A	1817:35	6.21°N
26 June 1966	8578A	1754:41	6.19°N
29 June 1966	8619A	1731:44	6.17°N

Table VI

MAGNETIC DIP ANGLE AT ALTITUDE 350 km OVER GEOGRAPHIC LOCATION 6.75°N, 100.66°E (SONGKHLA SITE DATA)

DATE	SATELLITE REVOLUTION NUMBER	TRANSVERSE POSITION (T_0) LOCAL TIME	MAGNETIC DIP ANGLE
4 Nov 1966	10374D	1154:56	5.83°S
6 Nov 1966	10395A	2347:39	5.97°S
8 Nov 1966	10436 A	2324:40	6.00°S
11 Nov 1966	10477A	2301:38	6.00°S
14 Nov 1966	10518A	2238:41	6.02°S
17 Nov 1966	10559A	2215:37	6.00°S
20 Nov 1966	10600A	2152:37	5.99°S
3 Dec 1966	10771D	0738:37	5.82°S
16 Dec 1966	10956A	1758:21	5.92°S
19 Dec 1966	10997A	1735:21	5.86°S

Table VII

MAGNETIC DIP ANGLE AT ALTITUDE 350 km

SATELLITE RECEIVING STATIONS	SUB-IONOSPHERIC POINT		MEAN MAGNETIC DIP ANGLE (I_B)	VARIANCE
	Longitude (λ_1)	Latitude (θ_1)		
Chiang Mai	99.21°E	20.33°N	25.47°N	0.06
Nakhon Sawan	100.60°E	16.54°N	16.59°N	0.08
Bangkok	100.60°E	14.38°N	12.33°N	0.08
Prachuap	100.47°E	12.14°N	6.20°N	0.02
Songkhla	100.66°E	6.75°N	5.94°S	0.07

The principal feature of magnetic dip angle is its linear variation with the geographic latitude near the geomagnetic dip equator. The estimated zero magnetic dip occurred directly above the geographic latitude of approximately 9.30°N (about 480 km south of Bangkok).

B. Comparison of Experimental and Theoretical Determination of Magnetic Dip Angle

To check the results of the magnetic dip angle at the ionospheric height obtained from the experimental Faraday rotation records, model calculations were made. The spherical harmonic function was chosen to represent the theoretical model of the geomagnetic field distribution. In addition, the surface magnetic dip angle measured in 1956-1966, by the Geodesy Department Ministry of Defense, Thailand[5] and the published NOO-CGS 1965 Chart 1700[6] were used to verify the applicability of the results.

The accuracy of the spherical harmonic function in modeling the geomagnetic field distribution depends primarily on the number of harmonics used The significant feature of the geomagnetic field can be accurately obtained by involving only the first six harmonics. However, this mathematical function cannot give any representation of the actual local variation of the geomagnetic field.

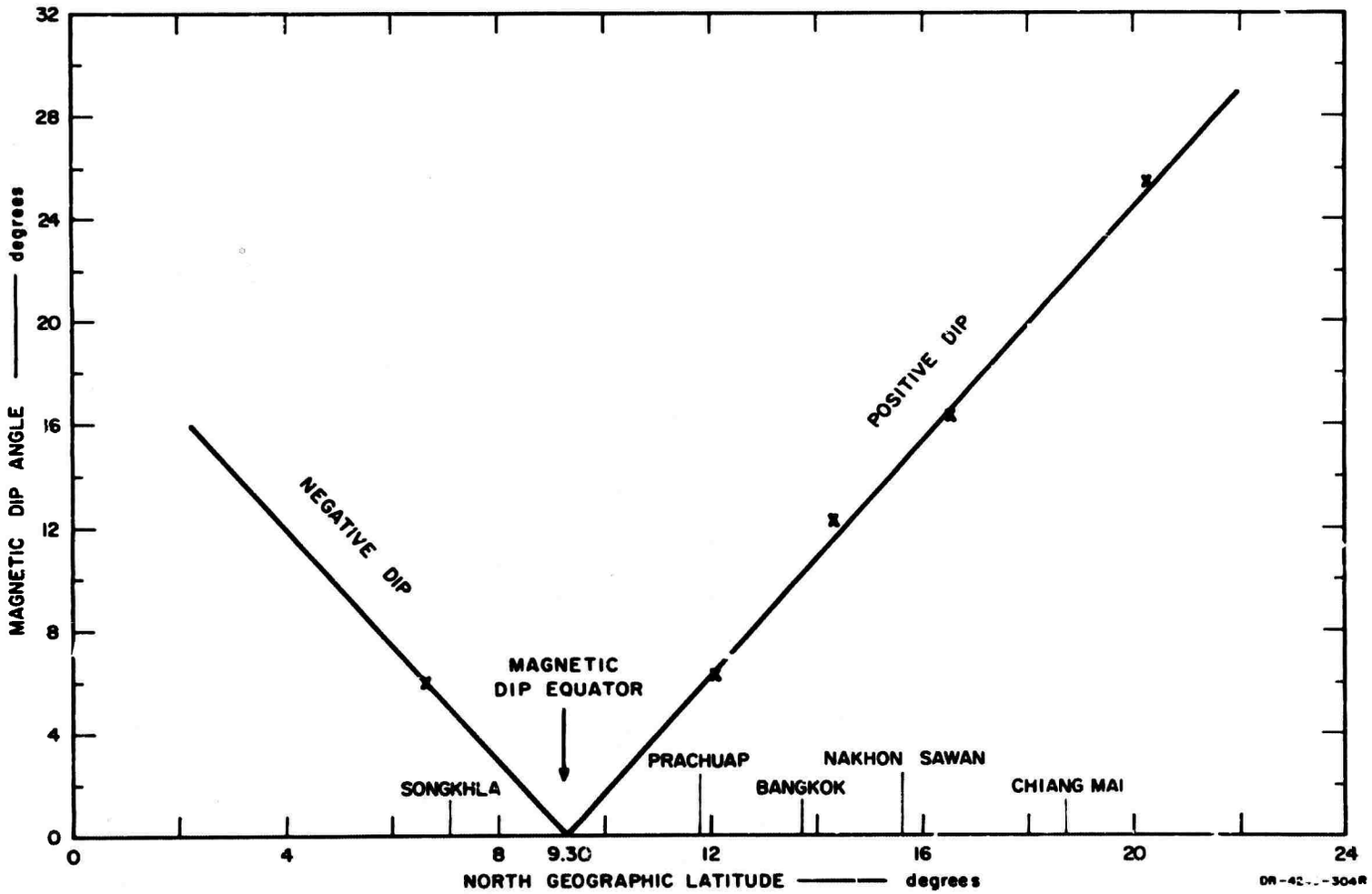

FIG. 8 MAGNETIC DIP ANGLE AT 350 km ALTITUDE

The comparison of the magnetic dip angle obtained from Faraday rotation technique with those derived from spherical harmonic function and other surface values is shown in Table VIII. The mean Faraday rotation technique values of the magnetic dip angle were taken from the data of Table VII. The surface measured values were obtained directly or interpolated for the corresponding sub-ionospheric points in Table VII. The surface published values were interpolated from NOO-CGS 1965 Chart 1700. The general feature of Table VIII is that the magnetic dip angle at the ionospheric height from Faraday rotation technique agrees surprisingly well with those surface values.

Table VIII

COMPARISON OF MAGNETIC DIP ANGLE

GEOGRAPHIC LOCATION		FARADAY ROTATION TECHNIQUE (h_c = 350 km)	SPHERICAL HARMONIC (h_c = 350 km)	MOD* SURFACE MEASUREMENTS	NOO-CGS$_2$ 1965 CHART SURFACE VALUE
Latitude	Longitude				
20.33°N	99.21°E	25.47°N	25.29°N	25.80°N	25.5°N
16.58°N	100.60°E	16.59°N	17.19°N	16.80°N	17.00°N
14.38°N	100.60°E	12.33°N	12.07°N	12.00°N	12.00°N
13.14°N	100.47°E	6.20°N	6.8°N	6.50°N	6.5°N
6.75°N	100.66°E	5.94°S	5.96°S	5.90°S	6.0°S

*Department of Geodesy, Ministry of Defense, Thailand.

C. Geomagnetic Dip Equator

A further result of this study is that the data are analyzed to obtain the location of geomagnetic dip equator at the ionospheric height. In this report the term geomagnetic dip equator means the locus where the magnetic dip angle is zero Table IX shows the estimated position of geomagnetic dip equator compared with estimates by other workers. All geographic locations of the geomagnetic dip equator contained in Table IX were obtained directly or interpolated from the data available to the author. In this table the geomagnetic dip equator estimates agree well, and the location of this equator at the ionospheric height is very close to the surface value.

Table IX

ESTIMATED POSITION OF GEOMAGNETIC
DIP EQUATOR NEAR 100°E

SOURCE	ALTITUDE (km)	GEOGRAPHIC LATITUDE
Author (1965-67)	350	9.30N
TEMPO (1963)[7]	100	9.40N
MOD (1956-66)[5]	0	9.40N
Vestine (1945)[17]	0	9.40N
NOO-CGS 1700 (1965)[6]	0	9.30N

The coincidence of the geomagnetic dip equator at ionospheric height and earth's surface for southeast Asia in the vicinity of longitude 100° east reveals that the earth's magnetic field is uniform in this region. Thus, the dipole field model is a good approximation of the earth's magnetic field for this region.

D. Accuracy of Results

A constant ionospheric centroid height was assumed for the position of the transverse propagation in the ionosphere, since at this point the magnetic dip angle was to be obtained. In reality, the ionospheric centroid height is not a constant value.[10] For a variation of centroid height of 50 km, errors in the values of magnetic dip angle and the corresponding subionospheric point of less than 3 percent will be introduced.

In this experiment, the time of the satellite at the transverse position was observed on analog chart records. The accuracy of this observation was limited by the width of the recorder marking lines. The smallest division of time on the marking scale was 5 seconds. The events time record can be resolved to within 1 second. The error due to the time reading is unlikely to exceed 2 percent.

Since the magnet declination in Thailand is small,[5] in the complete Eq. (A-16), this term is neglected for Eq. (11) to determine the magnetic dip angle. The error due to this approximation is less than 2 percent.

However, the total errors in the values of magnetic dip angle at the altitude of ionospheric centroid height obtained using the beacon satellite technique are usually less than 10 percent.

VI SUMMARY AND CONCLUSION

The use of simple instrumentation for Faraday rotation observations has provided a technique for calculating the magnetic dip angle over Thailand. The magnetic dip angle at ionospheric heights obtained from the Faraday rotation technique is very close to the surface value and compares well with values obtained by other workers. The results also have been compared with the spherical harmonic function with good agreement.

This technique proved useful for estimating the location of the geomagnetic dip equator which is located to the south of Bangkok. It is found that the location of this equator at ionospheric height is over the geographic latitude of 9.30N—about 480 km south of Bangkok. This value is very close to the surface value as obtained from several sources.

Knowledge of the coincidence of the magnetic dip angle at ionospheric height and the earth's surface indicates that the earth's magnetic field in Southeast Asia is uniform. This uniformity of the earth's magnetic field somewhat resembles that of a uniformly magnetized sphere, since this would conform with a simple dipole field. From this indication, a dipole field model is a good first-order approximation of the earth's magnetic field in the Southeast Asia region.

The results of the work presented in this report and the further analysis of these satellite data for their ionospheric data will give a potential of improvement in understanding of the radio propagation effects related to geomagnetic control of the ionosphere in Southeast Asia. Thus the simple instrumentation used for Faraday rotation observations can provide part of the ionospheric data base required for the study of equatorial radio communication.

APPENDIX A

DERIVATION OF MAGNETIC DIP ANGLE USING FARADAY ROTATION TECHNIQUE

BLANK PAGE

APPENDIX A

DERIVATION OF MAGNETIC DIP ANGLE USING FARADAY ROTATION TECHNIQUE

Assume no refraction in the ionosphere or lower atmosphere. Consider the geometry shown in Figs. A-1 and A-2 where the coordinates of points A (sub-satellite point), E (sub-satellite point), and R (ground station) are θ_s, λ_s; θ_i, λ_i; and θ_r, λ_r; geographic latitude and longitude, respectively. The earth's radius is denoted by R_e and the ionospheric centroid height is h_c. Satellite height is h_s.

By using spherical trigonometry,

$$\cos C = \sin \theta_s \sin \theta_r + \cos \theta_s \cos \theta_r \cos (\lambda_s - \lambda_r) \quad . \qquad \text{(A-1)}$$

Let the slant distance from satellite to ground station be equal to l

$$l = [R_e^2 + (R_e + h_s)^2 - 2R_e(R_e + h_s) \cos C]^{1/2} \quad . \qquad \text{(A-2)}$$

The inclination of signal ray, I_R, at the ionospheric centroid height can be determined as

$$\cot I_R = \frac{R_e(R_e + h_s) \sin C}{\{(R_e + h_c)^2[R_e^2 + (R_e + h_s)^2 - 2R_e(R_e + h_s) \cos C] - [R_e(R_e + h_s) \sin C]^2\}^{1/2}} \quad . \qquad \text{(A-3)}$$

From the ray-path geometry of Fig. A-1,

$$b = \cos^{-1}\left[\frac{R_e(R_e + h_s) \sin C}{(R_e + h_c)[R_e^2 + (R_e + h_s)^2 - 2R_e(R_e + h_s) \cos C]^{1/2}}\right] - \cos^{-1}\left[\frac{(R_e + h_s) \sin C}{[R_e^2 + (R_e + h_s)^2 - 2R_e(R_e + h_s) \cos C]^{1/2}}\right] \quad . \qquad \text{(A-4)}$$

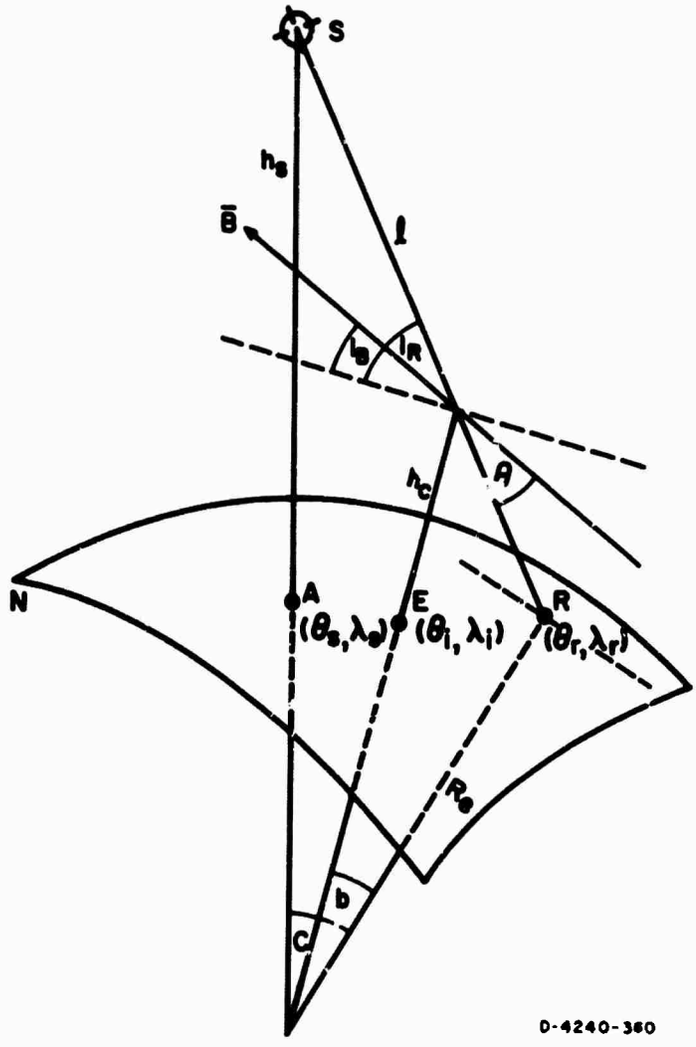

FIG. A-1 GEOMAGNETIC FIELD — RAY PATH GEOMETRY

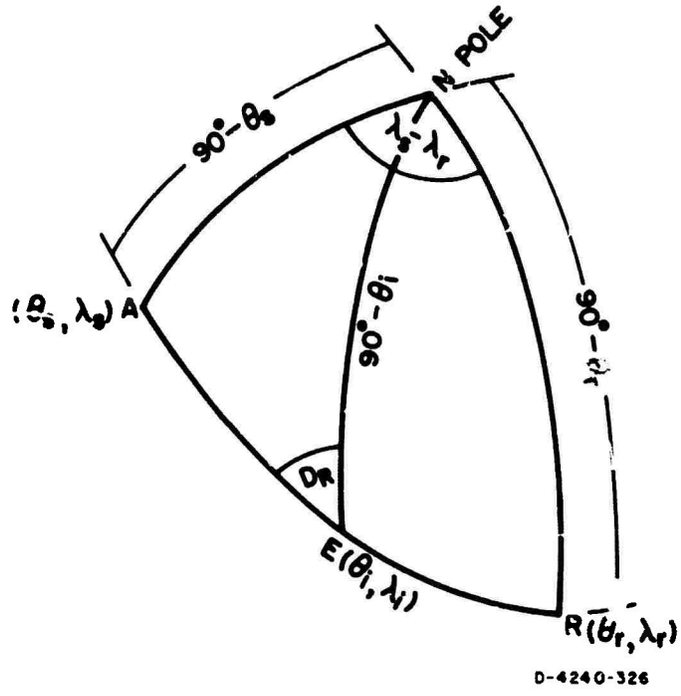

FIG. A-2 SURFACE ARC DISTANCE

Figure A-2 shows the arcs of the earth's surface from the geographical north pole to the sub-satellite point, sub-ionospheric point, and ground station. (If more convenient, we may join them to the geographical south pole.) Then the sub-ionospheric point $\iota(\theta_i,\lambda_i)$ is

$$\theta_i = \sin^{-1}\left[\sin\theta_r\,(\cos b - \sin b \cot C) + \sin\theta_s \sin b \operatorname{cosec} C\right] \tag{A-5}$$

$$\lambda_i = \lambda_r + N \qquad (\text{If } \lambda_s \geq \lambda_r) \tag{A-6}$$

$$\lambda_i = \lambda_r - N \qquad (\text{If } \lambda_s \leq \lambda_i) \tag{A-7}$$

where

$$N = \sin^{-1}\left\{\frac{\sin b}{\cos\theta_i}\left[1-\left(\frac{\sin\theta_s - \sin\theta_r\cos C}{\cos\theta_r \sin C}\right)^2\right]^{1/2}\right\} \quad . \tag{A-8}$$

The declination of the signal ray, D_R, at the ionospheric centroid height can be determined by

$$D_R = \cos^{-1}\left[\frac{\sin\theta_s}{\cos\theta_i \sin(C-b)} - \tan\theta_i \cot(C-b)\right] \quad . \qquad \text{(A-9)}$$

The angle between signal ray path and earth's magnetic field, θ, can be determined by the geometry as shown in Fig. A-3. Let OX, OY, and OZ be three perpendicular lines through the ionospheric centroid height at point O, where I_B and D_B are magnetic dip angle and declination, respectively. Using the direction cosines theorem,[18] the earth's magnetic field $\overline{OB}$ is in the direction with the direction cosines ($\cos\alpha_B$, $\cos\beta_B$, $\cos\gamma_B$), and the signal ray OS is in the directions ($\cos\alpha_R$, $\cos\beta_R$, $\cos\gamma_R$). By the rule for the addition of direction cosines, the angle, θ, between $\overline{OB}$ and OS can be determined by

$$\cos\theta = \cos\alpha_R \cos\alpha_B + \cos\beta_R \cos\beta_B + \cos\gamma_R \cos\gamma_B \quad . \qquad \text{(A-10)}$$

By the spherical trigonometry, we can solve for the cosine value as follows:

$$\begin{aligned} \cos\alpha_R &= \cos I_R \cos D_R \\ \cos\beta_R &= \cos I_R \sin D_R \\ \cos\gamma_R &= \sin I_R \end{aligned} \qquad \text{(A-11)}$$

and

$$\begin{aligned} \cos\alpha_B &= \cos I_B \cos D_B \\ \cos\beta_B &= \cos I_B \sin D_B \\ \cos\gamma_B &= \sin I_B \quad . \end{aligned} \qquad \text{(A-12)}$$

Substituting Eqs. (A-11) and (A-12) into (A-10),

$$\cos\theta = \cos I_R \cos I_B \cos(D_R - D_B) + \sin I_R \sin I_B \quad . \qquad \text{(A-13)}$$

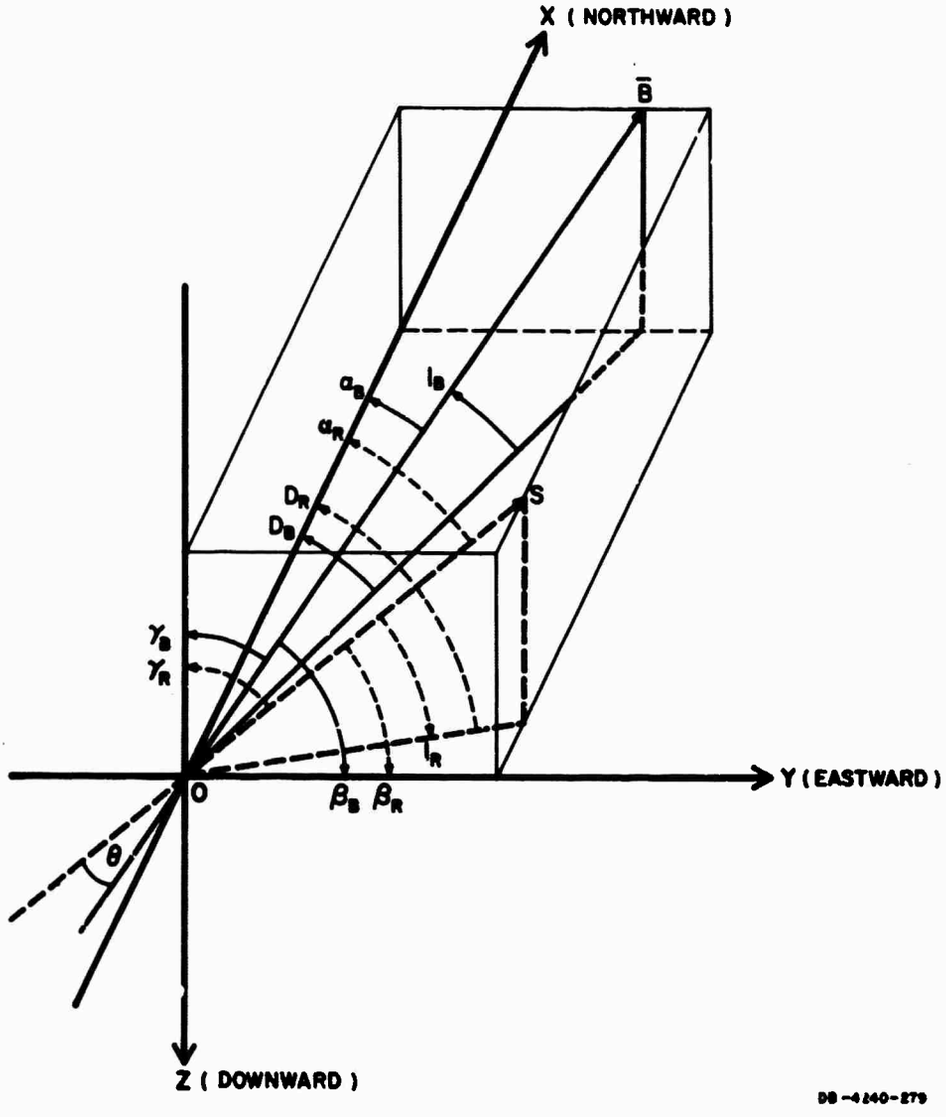

FIG. A-3 RECTANGULAR COORDINATE OF GEOMAGNETIC FIELD -- RAY PATH

Note that I_R, I_B is positive when the direction is below the horizontal. Since Fig. A-1 shows that I_R (direction of signal ray from satellite) is always negative, then Eq. (A-14) becomes

$$\cos \theta = \cos I_R \cos I_B \cos (D_R - D_B) - \sin I_R \sin I_B \quad . \qquad \text{(A-14)}$$

At the position where the signal ray from satellite is perpendicular to the earth's magnetic field, $\theta = 90°$, we have

$$\cos I_R \cos I_B \cos (D_R - D_B) - \sin I_R \sin I_B = 0 \qquad \text{(A-15)}$$

or

$$I_B = \tan^{-1} [\cot I_R \cos (D_R - D_B)] \quad . \qquad \text{(A-16)}$$

Since the magnetic declination, D_B, is small in Thailand (always less than 1 degree),[5] the approximation can be written as

$$\cos (D_R - D_B) \approx \cos D_R \quad . \qquad \text{(A-17)}$$

Then Eq. (A-16) can be rewritten with less than 2 percent error as

$$I_B = \tan^{-1} (\cot I_R \cos D_R) \quad . \qquad \text{(A-18)}$$

Equation (A-18) is used to calculate the magnetic dip angle above the earth's surface from the selected satellite fading records.

APPENDIX B

FIRST SIX SPHERICAL HARMONICS FOR THE GEOMAGNETIC FIELD

BLANK PAGE

APPENDIX B

FIRST SIX SPHERICAL HARMONICS FOR THE GEOMAGNETIC FIELD

$n = 1, m = 0$ to 1

$$x_1^0 = 0.3055 \sin \bar{\theta}$$

$$x_1^1 = \cos \bar{\theta} \, (0.0590 \sin \lambda - 0.0227 \cos \lambda)$$

$$\bar{X}_1 = x_1^0 + x_1^1$$

$$X_1 = \left(\frac{R_e}{R_e + h_c} \right)^3 \bar{X}_1$$

$n = 2, m = 0$ to 2

$$x_2^0 = 0.0228 \sin 2\bar{\theta}$$

$$x_2^1 = 1.7322 \cos 2\bar{\theta} \, (0.0303 \cos \lambda - 0.0190 \sin \lambda)$$

$$x_2^2 = 0.8661 \sin 2\bar{\theta} \, (0.0158 \cos 2\lambda + 0.0024 \sin 2\lambda)$$

$$\bar{X}_2 = x_2^0 + x_2^1 + x_2^2$$

$$X_2 = \left(\frac{R_e}{R_e + h_c} \right)^4 \bar{X}_2$$

$n = 3, m = 0$ to 3

$$x_3^0 = -0.00442 \, (5 \sin 3\bar{\theta} + \sin \bar{\theta})$$

$$x_3^1 = -0.30615 \, (5 \cos \bar{\theta} \cos 2\bar{\theta} - 10 \sin \bar{\theta} \sin 2\bar{\theta} + 3 \cos \bar{\theta})$$
$$\times \, [0.0191 \cos \lambda + 0.0045 \sin \lambda]$$

$$x_3^2 = 0.96825\,(2\sin\bar{\theta}\cos 2\bar{\theta} + \sin 2\bar{\theta}\cos\bar{\theta}) \times [0.0126\cos 2\lambda + 0.0029\sin 2\lambda]$$

$$x_3^3 = 2.3715\sin^2\bar{\theta}\cos\bar{\theta}\,[0.0091\cos 3\lambda - 0.0009\sin 3\lambda]$$

$$\bar{X}_3 = x_3^0 + x_3^1 + x_3^2 + x_3^3$$

$$X_3 = \left(\frac{R_e}{R_e + h_c}\right)^5 \bar{X}_3$$

<u>$n = 4,\ m = 0$ to 4</u>

$$x_4^0 = -0.00059\,(35\sin 4\bar{\theta} + 10\sin 2\bar{\theta})$$

$$x_4^1 = 5.5335\,[\cos^4\bar{\theta} - 3\sin^2\bar{\theta}\cos^2\bar{\theta} + 0.42857\,(\sin^2\bar{\theta} - \cos^2\bar{\theta})] \times [0.0080\cos\lambda + 0.0015\sin\lambda]$$

$$x_4^2 = 3.9112\,(2\cos^3\bar{\theta}\sin\bar{\theta} - 2\sin^3\bar{\theta}\cos\bar{\theta} - 0.14285\sin 2\bar{\theta}) \times [0.0058\cos 2\lambda - 0.0031\sin 2\lambda]$$

$$x_4^3 = -2.0895\,(3\cos^2\bar{\theta}\sin^2\bar{\theta} - \sin^4\bar{\theta}) \times [0.0038\cos 3\lambda + 0.0004\sin 3\lambda]$$

$$x_4^4 = 2.94\sin^3\bar{\theta}\cos\bar{\theta}\,[0.0031\cos 4\lambda - 0.0017\sin 4\lambda]$$

$$\bar{X}_4 = x_4^0 + x_4^1 + x_4^2 + x_4^3 + x_4^4$$

$$X_4 = \left(\frac{R_e}{R_e + h_c}\right)^6 \bar{X}_4$$

<u>$n = 5,\ m = 0$ to 5</u>

$$x_5^0 = 0.0001\,(63\sin 5\bar{\theta} + 21\sin 3\bar{\theta} + 6\sin\bar{\theta})$$

$$x_5^1 = 10.1626\,[\cos\bar{\theta}\,(\cos^4\bar{\theta} - 0.6666\cos^2\bar{\theta} + 0.0476) + \sin\bar{\theta}\,(0.6666\sin 2\bar{\theta} - 4\cos^3\bar{\theta}\sin\bar{\theta})] \times [0.0032\cos\lambda + 0.0002\sin\lambda]$$

$$x_5^2 = 7.6702\,(2\cos^4\bar{\theta}\sin\bar{\theta} - 3\sin^3\bar{\theta}\cos^2\bar{\theta} + 0.3333\sin^3\bar{\theta} - 0.6666\cos^2\bar{\theta}\sin\bar{\theta})[0.0020\cos 2\lambda + 0.0010\sin 2\lambda]$$

$$x_5^3 = -4.6777\,[3\sin^2\bar{\theta}\cos^3\bar{\theta} - 2\sin^4\bar{\theta}\cos\bar{\theta} - 0.3333\sin^2\bar{\theta}\cos\bar{\theta}] \times [0.0004\cos 3\lambda + 0.0005\sin 3\lambda]$$

$$x_5^4 = -2.1735\,(4\sin^3\bar{\theta}\cos^2\bar{\theta} - \sin^5\bar{\theta}) \times [0.0015\cos 4\lambda + 0.0014\sin 4\lambda]$$

$$x_5^5 = 3.3075\sin^4\bar{\theta}\cos\bar{\theta}\,[0.0009\sin 5\lambda - 0.0007\cos 5\lambda]$$

$$\bar{X}_5 = x_5^0 + x_5^1 + x_5^2 + x_5^3 + x_5^4 + x_5^5$$

$$X_5 = \left(\frac{R_e}{R_e + h_e}\right)^7 \bar{X}_5$$

<u>$n = 6$, $m = 0$ to 6</u>

$$x_6^0 = 0.01443\,(5.4545\cos^3\bar{\theta}\sin\bar{\theta} - 6\cos^5\bar{\theta}\sin\bar{\theta} - 0.4545\sin 2\bar{\theta})$$

$$x_6^1 = 18.8929\sin\bar{\theta}\,[(\cos^5\bar{\theta} - 0.909\cos^3\bar{\theta} + 0.1515) + \sin\bar{\theta}\,(2.7272\cos^2\bar{\theta}\sin\bar{\theta} - 5\cos^4\bar{\theta}\sin\bar{\theta})] \times [0.0005\cos\lambda - 0.0002\sin\lambda]$$

$$x_6^2 = 14.9428\,[\sin 2\bar{\theta}\,(\cos^4\bar{\theta} - 0.5454\cos^2\bar{\theta} + 0.0303) + \sin^2\bar{\theta}\,(0.5454\sin 2\bar{\theta} - 4\cos^3\bar{\theta}\sin\bar{\theta})] \times [0.0002\cos 2\lambda + 0.0011\sin 2\lambda]$$

$$x_6^3 = -9.8752\,[3\sin^2\bar{\theta}\cos\bar{\theta}\,(\cos^3\bar{\theta} - 0.2727\cos\bar{\theta}) + \sin^3\bar{\theta}\,(0.2727\sin\bar{\theta} - 3\cos^2\bar{\theta}\sin\bar{\theta})] \times [0.0024\cos 3\lambda]$$

$$x_6^4 = -5.4054\,[4\sin^3\bar{\theta}\cos\bar{\theta}\,(\cos^2\bar{\theta} - 0.0909) - \sin^4\bar{\theta}\sin 2\bar{\theta}] \times [0.0003\cos 4\lambda + 0.0001\sin 4\lambda]$$

$$x_6^5 = -2.2869\,[5\sin^4\bar{\theta}\cos^2\bar{\theta} - \sin^6\bar{\theta}]\,[0.0003\sin 5\lambda]$$

$$x_6^6 = -3.7422 \sin^5 \bar{\theta} \cos \bar{\theta} \, [0.0011 \cos 6\lambda + 0.0001 \sin 6\lambda]$$

$$\bar{X}_6 = x_6^0 + x_6^1 + x_6^2 + x_6^3 + x_6^4 + x_6^5 + x_6^6$$

$$X_6 = \left(\frac{R_e}{R_e + h_c} \right)^8 \bar{X}_6$$

$$X = X_1 + X_2 + X_3 + X_4 + X_5 + X_6$$

$n = 1, m = 1$

$$y_1^1 = -(0.0227 \sin \lambda + 0.059 \cos \lambda)$$

$$\bar{Y}_1 = y_1^1$$

$$Y_1 = \left(\frac{R_e}{R_e + h_c} \right)^3 \bar{Y}_1$$

$n = 2, m = 1$ to 2

$$y_2^1 = 1.7322 \cos \bar{\theta} \, (0.0303 \sin \lambda + 0.0190 \cos \lambda)$$

$$y_2^2 = 1.7322 \sin \bar{\theta} \, (0.0158 \sin 2\lambda - 0.0024 \cos 2\lambda)$$

$$\bar{Y}_2 = y_2^1 + y_2^2$$

$$Y_2 = \left(\frac{R_e}{R_e + h_c} \right)^4 \bar{Y}_2$$

$n = 3, m = 1$ to 3

$$y_3^1 = -0.30615 \, (5 \cos 2\bar{\theta} + 3)(0.0191 \sin \lambda - 0.0045 \cos \lambda)$$

$$y_3^2 = 1.9365 \sin 2\bar{\theta} \, (0.0126 \sin 2\lambda - 0.0029 \cos 2\lambda)$$

$$y_3^3 = 2.3715 \sin^2 \bar{\theta} \, (0.0091 \sin 3\lambda + 0.0009 \cos 3\lambda)$$

$$\bar{Y}_3 = y_3^1 + y_3^2 + y_3^3$$

$$Y_3 = \left(\frac{R_e}{R_e + h_c}\right)^5 \bar{Y}_3$$

$n = 4, m = 1$ to 4

$$y_4^1 = 5.5335\ (\cos^3 \bar{\theta} - 0.42857 \cos \bar{\theta})(0.008 \sin \lambda - 0.0015 \cos \lambda)$$

$$y_4^2 = 7.8224 \sin \bar{\theta}\ (\cos^2 \bar{\theta} - 0.14285) \times (0.0058 \sin 2\lambda + 0.0031 \cos 2\lambda)$$

$$y_4^3 = -6.2685 \sin^2 \bar{\theta} \cos \bar{\theta}\ (0.0038 \sin 3\lambda - 0.0004 \cos 3\lambda)$$

$$y_4^4 = 2.94 \sin^3 \bar{\theta}\ (0.0031 \sin 4\lambda + 0.0017 \cos 4\lambda)$$

$$\bar{Y}_4 = y_4^1 + y_4^2 + y_4^3 + y_4^4$$

$$Y_4 = \left(\frac{R_e}{R_e + h_c}\right)^6 \bar{Y}_4$$

$n = 5, m = 1$ to 5

$$y_5^1 = 10.1626\ (\cos^4 \bar{\theta} - 0.6666 \cos^2 \bar{\theta} + 0.0476) \times (0.0032 \sin \lambda - 0.0002 \cos \lambda)$$

$$y_5^2 = 15.3405 \sin \bar{\theta}\ (\cos^3 \bar{\theta} - 0.3333 \cos \bar{\theta}) \times (0.002 \sin 2\lambda - 0.001 \cos 2\lambda)$$

$$y_5^3 = -14.0331 \sin^2 \bar{\theta}\ (\cos^2 \bar{\theta} - 0.1111) \times (0.0004 \sin 3\lambda - 0.0005 \cos 3\lambda)$$

$$y_5^4 = -8.694 \sin^3 \bar{\theta} \cos \bar{\theta}\ (0.0015 \sin 4\lambda - 0.0014 \cos 4\lambda)$$

$$y_5^5 = -3.3075 \sin^4 \bar{\theta}\ (0.0007 \sin 5\lambda + 0.0009 \cos 5\lambda)$$

$$\bar{Y}_5 = y_5^1 + y_5^2 + y_5^3 + y_5^4 + y_5^5$$

$$Y_5 = \left(\frac{R_e}{R_e + h_c}\right)^7 \bar{Y}_5$$

$n = 6, m = 1$ to 6

$$y_6^1 = 18.8929 (\cos^5 \bar{\theta} - 0.909 \cos^3 \bar{\theta} + 0.1515) \times [0.0005 \sin \lambda + 0.0002 \cos \lambda]$$

$$y_6^2 = 29.8856 \sin \bar{\theta} (\cos^4 \bar{\theta} - 0.5454 \cos^2 \bar{\theta} + 0.0303) \times [0.0002 \sin 2\lambda - 0.0011 \cos 2\lambda]$$

$$y_6^3 = -29.6256 \sin^2 \bar{\theta} (\cos^3 \bar{\theta} \quad 0.2727 \cos \bar{\theta}) [0.0024 \sin 3\lambda]$$

$$y_6^4 = 21.6216 \sin^3 \bar{\theta} (\cos^2 \bar{\theta} - 0.0909) \times [0.0003 \sin 4\lambda - 0.0001 \cos 4\lambda]$$

$$y_6^5 = 11.4345 \sin^4 \bar{\theta} \cos \bar{\theta} [0.0003 \cos 5\lambda]$$

$$y_6^6 = -3.7422 \sin^5 \bar{\theta} [0.0011 \sin 6\lambda - 0.0001 \cos 6\lambda]$$

$$\bar{Y}_6 = y_6^1 + y_6^2 + y_6^3 + y_6^4 + y_6^5 + y_6^6$$

$$Y_6 = \left(\frac{R_e}{R_e + h_c}\right)^8 \bar{Y}_6$$

$$Y = Y_1 + Y_2 + Y_3 + Y_4 + Y_5 + Y_6$$

$n = 1, m = 0$ to 1

$$z_1^0 = 0.611 \cos \bar{\theta}$$

$$z_1^1 = 2 \sin \bar{\theta} (0.0227 \cos \lambda - 0.059 \sin \lambda)$$

$$\bar{Z}_1 = z_1^0 + z_1^1$$

$$Z_1 = \left(\frac{R_e}{R_e + h_c}\right)^3 \bar{Z}_1$$

$n = 2, m = 0$ to 2

$$z_2^0 = 0.0114 (3 \cos 2\bar{\theta} + 1)$$

$$z_2^1 = -2.5983 \sin 2\bar{\theta} (0.0303 \cos \lambda - 0.019 \sin \lambda)$$

$$z_2^2 = -2.5983 \sin^2 \bar{\theta} (0.0158 \cos 2\lambda + 0.0024 \sin 2\lambda)$$

$$\bar{Z}_2 = z_2^0 + z_2^1 + z_2^2$$

$$Z_2 = \left(\frac{R_e}{R_e + h_c}\right)^4 \bar{Z}_2$$

$n = 3, m = 0$ to 3

$$z_3^0 = -0.0059 (5 \cos^3 \bar{\theta} + 3 \cos \bar{\theta})$$

$$z_3^1 = 1.2246 \sin \bar{\theta} (5 \cos 2\bar{\theta} + 3)(0.0191 \cos \lambda + 0.0045 \sin \lambda)$$

$$z_3^2 = -3.873 \sin \bar{\theta} \sin 2\bar{\theta} (0.0126 \cos 2\lambda + 0.0029 \sin 2\lambda)$$

$$z_3^3 = -3.162 \sin^3 \bar{\theta} (0.0091 \cos 3\lambda - 0.0009 \sin 3\lambda)$$

$$\bar{Z}_3 = z_3^0 + z_3^1 + z_3^2 + z_3^3$$

$$Z_3 = \left(\frac{R_e}{R_e + h_c}\right)^5 \bar{Z}_3$$

$n = 4, m = 0$ to 4

$$z_4^0 = -0.00074 (35 \cos 4\bar{\theta} + 20 \cos 2\bar{\theta} + 9)$$

$$z_4^1 = -27.6675 \sin \bar{\theta} (\cos^3 \bar{\theta} - 0.42857 \cos \bar{\theta}) \times (0.008 \cos \lambda + 0.0015 \sin \lambda)$$

$$z_4^2 = -19.5562 \sin^2 \bar{\theta} (\cos^2 \bar{\theta} - 0.14285) \times (0.0058 \cos 2\lambda - 0.0031 \sin 2\lambda)$$

$$z_4^3 = 10.4475 \sin^3 \bar{\theta} \cos \bar{\theta} (0.0038 \cos 3\lambda + 0.0004 \sin 3\lambda)$$

$$z_4^4 = -3.675 \sin^4 \bar{\theta} (0.0031 \cos 4\lambda - 0.0017 \sin 4\lambda)$$

$$\bar{Z}_4 = z_4^0 + z_4^1 + z_4^2 + z_4^3 + z_4^4$$

$$Z_4 = \left(\frac{R_e}{R_e + h_c}\right)^6 \bar{Z}_4$$

$n = 5$, $m = 0$ to 5

$$z_5^0 = 0.00013\,(63\cos 5\bar{\theta} + 35\cos 3\bar{\theta} + 30\cos\bar{\theta})$$

$$z_5^1 = -60.9756\sin\bar{\theta}\,(\cos^4\bar{\theta} - 0.6396\cos^2\bar{\theta} + 0.0476) \times (0.0032\cos\lambda + 0.0002\sin\lambda)$$

$$z_5^2 = -46.0215\sin^2\bar{\theta}\,(\cos^3\bar{\theta} - 0.3333\cos\bar{\theta}) \times (0.002\cos 2\lambda + 0.001\sin 2\lambda)$$

$$z_5^3 = 28.0662\sin^3\bar{\theta}\,(\cos^2\bar{\theta} - 0.1111) \times (0.0004\cos 3\lambda + 0.0005\sin 3\lambda)$$

$$z_5^4 = 13.041\sin^4\bar{\theta}\cos\theta\,(0.0015\cos 4\lambda + 0.0014\sin 4\lambda)$$

$$z_5^5 = 3.969\sin^5\bar{\theta}\,(0.0007\cos 5\lambda - 0.0009\sin 5\lambda)$$

$$\bar{Z}_5 = z_5^0 + z_5^1 + z_5^2 + z_5^3 + z_5^4 + z_5^5$$

$$Z_5 = \left(\frac{R_e}{R_e + h_c}\right)^7 \bar{Z}_5$$

$n = 6$, $m = 0$ to 6

$$z_6^0 = -0.10106\,(\cos^6\bar{\theta} - 1.3636\cos^4\bar{\theta} + 0.4545\cos^2\bar{\theta} - 0.0216)$$

$$z_6^1 = -132.25\sin\bar{\theta}\,(\cos^5\bar{\theta} - 0.909\cos^3\bar{\theta} + 0.1515) \times (0.0005\cos\lambda - 0.0002\sin\lambda)$$

$$z_6^2 = -104.5996\sin^2\bar{\theta}\,(\cos^4\bar{\theta} - 0.5454\cos^2\bar{\theta} + 0.0303) \times (0.0002\cos 2\lambda + 0.0011\sin 2\lambda)$$

$$z_6^3 = 69.1264\sin^3\bar{\theta}\,(\cos^3\bar{\theta} - 0.2727\cos\bar{\theta})(0.0024\cos 3\lambda)$$

$$z_6^4 = 37.8378\sin^4\bar{\theta}\,(\cos^2\bar{\theta} - 0.0909) \times (0.0003\cos 4\lambda + 0.0001\sin 4\lambda)$$

$$z_6^5 = 16.0083 \sin^5 \bar{\theta} \cos \bar{\theta} \, (0.0003 \sin 5\lambda)$$

$$z_6^6 = 4.3659 \sin^6 \bar{\theta} \, (0.0011 \cos 6\lambda + 0.0001 \sin 6\lambda)$$

$$\bar{Z}_6 = z_6^0 + z_6^1 + z_6^2 + z_6^3 + z_6^4 + z_6^5 + z_6^6$$

$$Z_6 = \left(\frac{R_e}{R_e + h_c} \right)^8 \bar{Z}_6$$

$$Z = Z_1 + Z_2 + Z_3 + Z_4 + Z_5 + Z_6$$

$$B = [(X)^2 + (Y)^2 + (Z)^2]^{1/2}$$

$$H = [(X)^2 + (Y)^2]^{1/2}$$

$$I_B = \text{arc tan } Z/H$$

$$D_B = \text{arc tan } Y/H$$

REFERENCES

1. Vichai T. Nimit, Boonaong Punyarut, Clifford L. Rufenach, "Faraday Rotation Data: Bangkok, Thailand, Reporting period: November 1964-June 1965," Geophysical Data Report, SRI Project 4240, Contract DA-36-039 AMC-00040(E), Stanford Research Institute, Menlo Park, California.

2. Vichai, T. Nimit, Boonsong Punyarut, Clifford L. Rufenback, "Faraday Rotation Data: Bangkok, Thailand, Reporting period: July-December 1965," Geophysical Data Report, SRI Project 4240, Contract DA-36-039 AMC-00040(E), Stanford Research Institute, Menlo Park, California.

3. Vichai T. Nimit, "Faraday Rotation Data: Bangkok, Thailand Reporting period: January-June 1966," Geophysical Data Report, SRI Project 4240, Contract DA-36-039 AMC-00040(E), Stanford Reaearch Institute, Menlo Park, California.

4. Vichai T. Nimit, "Faraday Rotation Data: Bangkok, Thailand Reporting period: July-December 1966," Geophysical Data Report, SRI Project 4240, Contract DA-36-039 AMC-00040(E), Stanford Research Institute, Menlo Park, California.

5. Private Communication with the Geodesy Department, Ministry of Defense, Bangkok. Thailand.

6. U.S. Navy Oceanographic Office-U.S. Coast and Geodetic Survey, "The Magnetic Inclination or Dip for the Year 1965," 1700.

7. Walter F. Dudziak, David D. Kleinecke, and Theodore J. Koatigen, "Graphical Diaplays of Geomagnetic Geometry," RM63 TMP-2, DASA 1372, Contract DA 490146-XZ-109 Technical Military Planning Operation, General Electric Company, Santa Barbara, California, p. 51 (1 April 1963).

8. George Hagn, "Orientation of Linearly Polarized HF Antennas for Short-Path Communication via the Ionosphere Near the Geomagnetic Equator," Research Memorandum 5 (Revised), SRI Project 4240, Contract DA-36-039 AMC-00040(E), Stanford Research Institute, Menlo Park, California (Reviaed June 1964).

9. Clifford L. Rufenach, Vichai T. Nimit and Robert E. Leo, "Faraday Rotation Measurements of Electron Content near the Magnetic Equator, Uaing the Tranait IV-A Satellite," Special Technical Report 14, Contract DA-36-039 AMC-00040(E), SRI Project 4240, Stanford Reaearch Inatitute, Menlo Park, California, pp. 1-8 (January 1966).

10. K. Daviea, "Ionospheric Radio Propagation," NBS Monograph 80, pp. 125-129, National Bureau of Standarda, Boulder, Colorado (April 1965).

11. O. K. Garriott and F. de Mendonca, "A Compariaon of Methods Used for Obtaining Electron Content from Satellite Observations," *J. Geophys. Research*, Vol. 68, pp. 4917-4927 (1963).

12. K. C. Yeh and V. H. Gonzales, "Note on th Geometry of the Earth's Magnetic Field Uaeful to Faraday Effect Experiments," *J. Geophys. Research*, Vol. 65, pp. 3209-3214 (1960).

13. S. Chapman and J. Bartela, *Geomagnetism*, Vol. II, pp. 604-637 (Oxford University Preas, 1940).

14. C. R. Wylie, *Advanced Engineering Mathematics*, pp. 449-459 (McGraw-Hill Book Company, Inc., 1960).

15. H. F. Finch, B. R. Leaton, "The Earth's Main Magnetic Field Epoch 1955," *Monthly Notices Roy. Astron. Soc., Geophys.*, Suppl. 7, pp. 314 (1957).

16. George Hagn, "Abaorption of Ionospherically Propagated HF Radio Waves Under Conditions Where the Quaai-Transve.se (QT) Approximation ia Valid," Special Technical Report 9, SRI Project 4240, Contract DA-36-039 AMC-00040(E), Stanford Research Institute, Menlo Park, California (September 1965).

17. E. H. Vestine, *et al.*, "Carnegie Inst. Wash. Publ., 580," pp. 1-27 (1947).

18. H. V. Lovry and H. A. Hayden, *Advanced Mathematics for Technical Students*. Vol. II, pp. 211-227 (Longmans, Green and Co. Ltd., 1960).

UNCLASSIFIED

Security Classification

DOCUMENT CONTROL DATA - R & D

(Security classification of title, body of abstract and indexing annotation must be entered when the overall report is classified)

1. ORIGINATING ACTIVITY (Corporate author) Stanford Research Institute 333 Ravenswood Avenue Menlo Park, California	2a. REPORT SECURITY CLASSIFICATION UNCLASSIFIED 2b. GROUP N/A

3. REPORT TITLE

MEASUREMENT OF EQUATORIAL MAGNETIC DIP ANGLE AT IONOSPHERIC HEIGHTS

4. DESCRIPTIVE NOTES (Type of report and inclusive dates)

Special Technical Report 33

5. AUTHOR(S) (First name, middle initial, last name)

Vichai T. Nimit

6. REPORT DATE May 1967	7a. TOTAL NO. OF PAGES 64	7b. NO. OF REFS 18
8a. CONTRACT OR GRANT NO. DA-36-039 AMC-00040(E) b. PROJECT NO. c. d.	9a. ORIGINATOR'S REPORT NUMBER(S) STR 33 SRI Project 4240 9b. OTHER REPORT NO(S) (Any other numbers that may be assigned this report) ARPA Order 371	

10. DISTRIBUTION STATEMENT

Distribution of this document is unlimited

11. SUPPLEMENTARY NOTES	12. SPONSORING MILITARY ACTIVITY Advanced Research Projects Agency Washington, D.C.

13. ABSTRACT

Data collected for calculating electron content of the ionosphere by the Faraday rotation technique can be used to calculate the magnetic dip angle at ionospheric height near the geomagnetic dip equator. In this report the magnetic dip angle at ionospheric height was determined at the position where the angle between the ray path from the satellite to the ground station and the geomagnetic field vector is 90° (transverse position).

The magnetic dip angle calculation was based on the assumption of a constant height of 350 km for the centroid of the ionospheric electron-density profile. The spherical harmonic analysis is used to verify the experimental results. The results compare well with the surface magnetic dip angle, measured in 1956-1960 by the Geodesy Department of the Ministry of Defense, Thailand, and indicate that the magnetic dip angle at ionospheric height is very close to the surface value.

These data permit estimation of the position of the geomagnetic dip equator at the ionospheric height. The estimated position of this equator is directly above the geographic latitude of 9.30°N. This latitude intersects the southern peninsula of Thailand about 480 km south of Bangkok (near Surat Thani). This estimated value compares well with the surface geomagnetic dip equator and indicates that the dipole field is a good model for Southeast Asia in the vicinity of longitude 100°E.

DD FORM 1 NOV 68 1473 (PAGE 1)

S/N 0101-807-6801

UNCLASSIFIED

Security Classification

14 KEY WORDS	LINK A		LINK B		LINK C	
	ROLE	WT	ROLE	WT	ROLE	WT
Geomagnetic Dip Equator						
Geomagnetic Dip Angle						
Satellite						
Explorer 22 (S-66)						
Faraday Rotation Records						
Spherical Harmonic Analysis						
Thailand						
SEACORE						